Available online at www.sciencedirect.com
SCIENCE DIRECT®
ELSEVIER
European Journal of Mechanics B/Fluids 21 (2002) 561–577

Focusing of edge waves above a sloping beach

Andrey Kurkin [a], Efim Pelinovsky [b]

[a] Department of Applied Mathematics, Nizhny Novgorod State Technical University, 24 Minin Street, Nizhny Novgorod, Russia
[b] Laboratory of Hydrophysics and Nonlinear Acoustics, Institute of Applied Physics, 46 Uljanov Street, Nizhny Novgorod, Russia

Received 5 April 2002; received in revised form 9 July 2002; accepted 16 July 2002

Abstract

The mechanism of the spatial-temporal focusing (dispersion enhancement) of the edge waves in the shelf zone is studied in the framework of linear shallow water theory. The multi-modal Stokes edge waves are considered as an example of the shallow waves propagated in the coastal zone above uniformly sloping plane beach. The method to find the localized anomalous high wave generated in the process of the wave packet focusing is suggested. The characteristics of the wave trains evolving into the anomalous large wave are discussed.

1. Introduction

Wave propagation in the inhomogeneous medium can induce the scattering of the wave energy, as well as its capturing. The last phenomenon has a great interest due to the weak attenuation of the waves over long distances. There is a lot of tsunami observations when strong intensity can be explained with the theory of the trapped waves only. For instance, Ishi and Abe [1] suggested that the manifestation of the catastrophic 1952 Kamchatka tsunami on the Japanese coast is related with the trapped waves. Due to frequency dispersion of the trapped waves, such waves approach significantly later then the leading wave, and their amplitudes are significantly higher. The existing of the trapped waves explains the non-uniform character of the tsunami height along the coastline [2,3]. Totally, approximately 70% of the tsunami wave energy propagates along the Kurile Islands in Pacific as the trapped waves [4]. Coastally trapped waves are an important component in the sea disturbances produced by cyclones moving along coastlines [5]. Edge waves may be generated from normally incident wind waves due to strong nonlinearity of the wind waves [6–8]. Several pictures of edge waves are available in book by Komar [9].

The modal structure of the linear barotropic trapped waves in a basin of variable depth is described in papers [10–14] and books [15,16]. Usually, the kinematic properties of those waves are studied because the dispersion relations can be detected from the observations using the spectrum analysis. More difficult is to determine the energetic characteristics of the trapped waves related with their sources and sinks on large oceanic areas. A popular model of the generation of the background trapped waves is the atmospheric model with variable atmospheric pressure and wind stress, see, for instance [16]. This model is applied usually for description of the mesoscale ocean response on the atmospheric disturbances. Impulse generation of the trapped waves can be related with underwater earthquakes and volcano eruptions, fast and large-scale variations of the atmospheric conditions. Usually, the source acts during the short time resulting to the wave generation, and the solution of the classical Cauchy problem for the linear or nonlinear wave equation is a typical mathematical task in the theory of wave propagation. Sometimes, the wave generation can be related with multiple sources during the relative short intervals. For instance, the tsunami generation at the Virginia Islands during the 1867 earthquake is described as “A great sea wave was started by the first shock, an second larger one by the second shock some ten minutes later; other waves followed but were relatively unimportant” [17]. Multi-generation

E-mail address: enpeli@hydro.appl.sci-nnov.ru (E. Pelinovsky).

PII: S0997-7546(02)01201-3

of the intense wave groups due to nonlinearity and dispersion may induce the wave interaction with formation of the anomalous high waves. These processes have never been studied for the trapped waves.

Meanwhile, such processes called as freak or rogue wave phenomena are known for the wind waves in the ocean. Freak waves appeared and disappeared very rapidly on relative still sea surface. Twenty two supercarriers were lost due to collision with freak waves during 1969–1994 [18]. The freak wave with height 26 m was recorded on the oil platform in the North Sea in 1995 [19]. The importance of the extreme wave forecasting induced the developing of the theoretical models taken into account the wave-current interaction, dispersive and geometrical focusing, nonlinear instabilities [20–32]. Of course, the mathematics of short-scale wind waves differs from the mathematics of the large-scale wave motion, but the physical processes related with dispersion and nonlinearity can play the same role in both cases. The goal of this paper is to discuss the mechanism of spatial-temporal focusing of the edge waves in a basin of variable depth. In the case when long shelf waves are generated by nonlinear interaction of the wind wave groups propagated to the shore [7,8] the origin of the large-scale anomalous wave is related with the wind as for the freak waves in the open sea. The paper is organized as following. The modal structure of the Stokes edge waves above the plane beach is reproduced in Section 2. The physics of the wave focusing is discussed in Section 3 in the framework of the kinematic model for slowly modulated edge wave trains. The exact and approximated solutions of the linear shallow water system for the anomalous impulse forming in the one-modal Stokes edge wave field are given in Section 4. Multi-modal large-amplitude Stokes edge waves are discussed in Section 5. Obtained results are summarized in conclusion.

2. Stokes edge waves on the plane beach

The Stokes edge waves as is well-known are the waves propagated along the plane beach. The linear theory of the Stokes edge waves is well described, see, for instance, LeBlond and Mysak [15], Rabinovich [16]. Minzoni and Whitham [33] show that within the framework of edge wave theory the linearisation of governing equations and that of the shallow water equations are both equally consistent. Let us consider the wave motion above the cylindrical bottom in the framework of the linear shallow water theory only

$$\frac{\partial \eta}{\partial t} + \frac{\partial}{\partial x}\big(h(y)u\big) + \frac{\partial}{\partial y}\big(h(y)v\big) = 0, \tag{1}$$

$$\frac{\partial u}{\partial t} + g\frac{\partial \eta}{\partial x} = 0, \qquad \frac{\partial v}{\partial t} + g\frac{\partial \eta}{\partial y} = 0, \tag{2}$$

where $\eta(x, y, t)$ is the surface displacement, u and v are the alongshore and offshore components of the horizontal current, g is the gravity acceleration, $h = \alpha y$ is the water depth, y is the offshore coordinate and x is the alongshore coordinate, α is the constant bottom slope. The system (1)–(2) can be reduced to the wave equation for the surface displacement

$$\frac{\partial^2 \eta}{\partial t^2} - g \cdot \mathrm{div}(h\nabla\eta) = 0. \tag{3}$$

The boundary conditions (on offshore coordinate) correspond to the wave vanishing on infinity and its bounding on the shoreline. Separating the variables in (3), the structure of the free Stokes edge waves is presented in explicit form

$$\eta_n(x, y, t) = A_n \exp(-ky) L_n(2ky) \exp\big(\mathrm{i}(\omega_n t - kx)\big), \tag{4}$$

where L_n is the Laguerre polynomial described the offshore modal structure; the frequency, ω and along wave number, k are satisfied to the dispersion relation

$$\omega_n = \sqrt{(2n+1)\alpha g k}, \tag{5}$$

n is the integer indicated the modal number, and A_n is the wave amplitude (in general, complex value).

The velocity field in the Stokes edge wave is expresses as

$$u_n(x, y, t) = A_n \frac{gk}{\omega_n} \exp(-ky) L_n(2ky) \exp\big(\mathrm{i}(\omega_n t - kx)\big), \tag{6}$$

$$v_n(x, y, t) = \mathrm{i} A_n \frac{g}{\omega_n} \frac{\mathrm{d}}{\mathrm{d}y}\big[\exp(-ky) L_n(2ky)\big] \exp\big(\mathrm{i}(\omega_n t - kx)\big). \tag{7}$$

The Laguerre polynomials tend to zero on infinity, thus the wave field is concentrated in the coastal zone. The offshore structure of the water displacement in the Stokes edge waves is shown in Fig. 1. The wave field is rapidly decreasing with distance from the beach. Weak oscillations (less then 25% of maximal value) are spreading in deep water when the mode number increases (in the framework of shallow water theory).

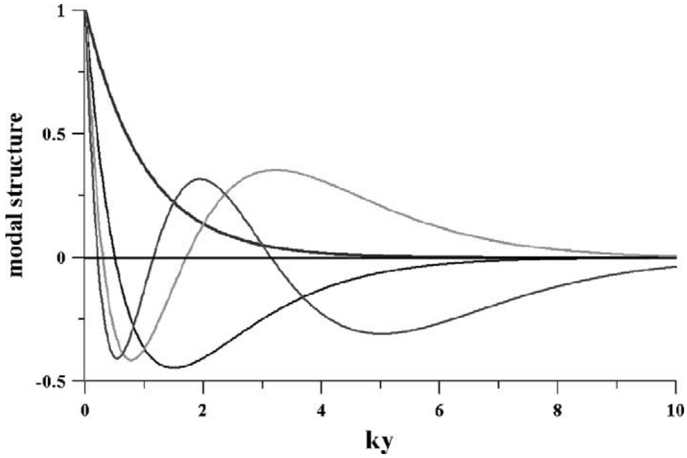

Fig. 1. Offshore structure of the shallow Stokes edge waves.

The wave equation (3) should be solved with the initial conditions. For tsunami problem the piston model is the popular model, thus the initial conditions correspond to the initial displacement of the sea surface

$$\eta(x,y,t=0)=\eta_0(x,y), \qquad \frac{\partial\eta}{\partial t}(x,y,t=0)=0, \tag{8}$$

but other initial conditions can be easily considered due to linearity of the wave equation. The solution of the Cauchy problem for Eq. (3) can be expressed in the integral form. Physically, this solution is presented as a sum of the near field (algebraically attenuated from the source) and the wave component given the superposition of the Stokes edge waves (4). Far from the source, the wave component contributes mainly in the resulting field. As in existing models of the freak wave formation, we will consider the trapped waves far from the source and ignore the near field. The wave component of the general solution presents by the Fourier series,

$$\eta(x,y,t)=\sum_{n=0}^{n=\infty}\int_{-\infty}^{+\infty} A_n(k)\exp\bigl(-|k|y\bigr)L_n\bigl(2|k|y\bigr)\exp\bigl(\mathrm{i}(\omega_n t-kx)\bigr)\,\mathrm{d}k, \tag{9}$$

where

$$A_n(k)=\frac{k}{\pi}\int_0^{+\infty}\exp\bigl(-|k|y\bigr)L_n\bigl(2|k|y\bigr)\,\mathrm{d}y\int_{-\infty}^{+\infty}\eta_0(x,y)\exp(\mathrm{i}kx)\,\mathrm{d}x. \tag{10}$$

Thus, the linear superposition of the free Stokes edge waves (9) is the mathematical model for discussion of the anomalous high wave appearance.

It is important to note that the Stokes edge waves have significant dispersion; their dispersion relation (5) coincides with the dispersion relation for the wind waves in deep water (with reduced value of the gravity acceleration). Nonlinear correction to the edge wave has been obtained by Whitham [34] showing that the edge wave is modulational unstable like the Benjamin–Feir instability. As a result, nonlinear Schrödinger equation can be derived for the envelope of the quasi-monochromatic wave packet, it has the same form as for waves in deep water with reduction of the gravity acceleration [35,36]. The appearance of the freak wave in the framework of the cubic nonlinear Schrödinger equation is predicted by many authors [22–24,26,27,30]. Due to the same mathematical model, the edge wave train will generate anomalous high impulse, and there is not necessary to repeat here the corresponding results for narrow spectrum. More interesting features of the Stokes edge waves are its wide spectrum and the multi-modal character of the wave propagation. Nonlinear interaction of the Stokes edge waves with different modal structures is studied by Kenyon [37], Kochergin and Pelinovsky [38] and Kirby et al. [39]. Although the kinematic conditions of the resonance interactions are satisfied for the Stokes edge waves propagated in any directions, but the coefficients of the nonlinear interactions differ from zero for counter-propagating waves only [39]. Such interactions in all directions are important for climate processes and equilibrium of the wave field. For collinear Stokes edge waves the coefficients of the nonlinear interactions are equal to zero [39], and it means that the interaction between different modes of the collinear Stokes edge waves can be ignored. The freak wave phenomenon is not trivial mainly for collinear waves, because the interaction of the counter-propagating waves leads to appearance of the large pulse with double amplitudes as a minimum. So, the linear superposition of the collinear Stokes edge waves with different modal numbers is the good approximated solution in a weak nonlinear limit.

3. Dispersive mechanism of the appearance of large amplitude waves

In the framework of the linear theory the appearance of the large-amplitude waves may be explained by a focusing mechanism. Usually, the wave focusing is related with geometrical factors, as well as with wave dispersion. The Stokes edge waves are unidirectional waves and, therefore, the geometrical focusing here is impossible. Dispersion is usually considered as the mechanism of the wave attenuation due to transformation of the initial impulse into the wave train with decreasing amplitude and increasing length. It is evident that if at the initial moment the wave packet has the slow waves in its front and the fast waves on its end, the fast waves will overtake the slow waves. In the moment of overtaking (wave focus) the individual waves merge with forming of the large amplitude impulse. If the Stokes wave represents the quasi-monochromatic wave train with slowly variable amplitude, $A(x,t)$ and wave number, $k(x,t)$, then this process can be described by the well-known kinematic equations [20,40,41]

$$\frac{\partial k}{\partial t}+c_{\mathrm{gr}}(k)\frac{\partial k}{\partial x}=0, \tag{11}$$

$$\frac{\partial A^2}{\partial t}+\frac{\partial}{\partial x}\left(c_{\mathrm{gr}}(k)A^2\right)=0, \tag{12}$$

where the group velocity, c_{gr} is calculated from the dispersion relation (5). These equations are valid for each mode of the Stokes edge waves. Note that the kinematic equations are one-dimensional equations in spite of two-dimensional character of the edge waves. The first kinematic equation (11) can be re-written as an equation for the group velocity, $c_{\mathrm{gr}}=\mathrm{d}\omega/\mathrm{d}k$ after multiplying on $\mathrm{d}c_{\mathrm{gr}}/\mathrm{d}k$

$$\frac{\partial c_{\mathrm{gr}}}{\partial t}+c_{\mathrm{gr}}\frac{\partial c_{\mathrm{gr}}}{\partial x}=0. \tag{13}$$

The nonlinear hyperbolic system (12) and (13) is solved exactly

$$c_{\mathrm{gr}}(x,t)=c_0(\xi)=c_0(x-c_{\mathrm{gr}}t), \tag{14}$$

$$A(x,t)=\frac{A_0(\xi)}{\sqrt{1+t(\mathrm{d}c_0/\mathrm{d}\xi)}}, \tag{15}$$

for any initial distributions, $c_0(x)$ and $A_0(x)$. Here $\xi=x-c_{\mathrm{gr}}t$ is moving coordinate. The first solution (14) has plain physical sense: each quasi-monochromatic wave packet propagates with own group speed, and there is no interaction between different wave packets in the linear problem. The second equation (15) shows, in fact, the spatial variability of the wave packet density. If the fast wave are behind the slow waves at the initial time, then $\mathrm{d}c_0/\mathrm{d}x<0$, and from (15) follows the amplification of the wave energy in the place of the wave concentration. At the focusing time

$$T=\frac{1}{(-\mathrm{d}c_0/\mathrm{d}x)_{\max}}, \tag{16}$$

the wave amplitude becomes infinity. Then the fast waves move forward and the wave amplitude decreases again. This simplified model is not valid, unfortunately, in the vicinity of the wave focus, because the approximation of slowly varied amplitude breaks down at the focal point (several wave packets meet in the same point). But the kinematic model demonstrates the focusing process very well, and also the reversibility of the focusing process and dispersive attenuation process.

So, the focusing process is the inverse process of the dispersive attenuation. Mathematically, it follows from the invariance of the wave equation (3) on the sign changing of time and coordinates (in fact, only the propagated coordinate, alongshore coordinate should be considered). Therefore, the complicated mathematical problem to prove the appearance of the anomalous impulse from the given wave field can be reduced to the simpler Cauchy problem of the evolution of the anomalous impulse. All obtained solutions after inverting in space will present the wave packets evolved into the anomalous high impulse.

More realistic model for the quasi-harmonic wave train evolution is based on the parabolic equation considered by Pelinovsky et al. [28] for waves above flat bottom,

$$\mathrm{i}\frac{\partial A}{\partial t}=\frac{1}{2}\frac{\mathrm{d}^2\omega}{\mathrm{d}k^2}\frac{\partial^2 A}{\partial x^2}, \tag{17}$$

where again the dispersion relation (5) is used. This equation is also one-dimensional, in spite of the two-dimensional character of the edge wave structure. The process of the wave focusing takes place as in the framework of the kinematic equations, but in the vicinity of the focal point, the maximal amplitude is bounded [28]. The invariance of the parabolic equation (17) is evident, so, the scheme of calculation of the anomalous high wave described above “works” also in this model. The nonlinearity of the quasi-harmonic Stokes edge wave train leads to additional cubic nonlinear term in (17), and the corresponding nonlinear

Schrödinger equation derived by Akylas [35] and Yeh [36]. The dynamics of the appearance of the freak wave in the framework of the nonlinear Schrödinger equation is well studied [22–24,26,27,30], so, the process of the focusing of the quasi-harmonic wave packets seems to be evident. The influence of the offshore coordinate leads only to wave decreasing according to (4) with the constant carrier wave number k. In next sections, the appearance of the high amplitude impulse in the Stokes edge wave filed with the wide spectrum will be investigated.

4. Anomalous impulse forming in the one-modal Stokes edge wave field

First of all, the wave focusing of the first mode ($n = 0$) of the Stokes edge wave will be analyzed. In this case the Laguerre polynomial is the trivial constant ($L_0(y) = 1$) and the wave evolution is described by the Fourier integral

$$\eta(x, y, t) = \int A(k) \exp\bigl(\mathrm{i}(\omega t - kx) - |k|y\bigr)\,\mathrm{d}k \tag{18}$$

with the dispersion relation

$$\omega = \sqrt{g\alpha|k|}\,\operatorname{sign} k \tag{19}$$

and the condition, $A(-k) = A^*(k)$ ensues that the wave field is real.

As it is known, Eqs. (18) and (19) are valid for the Stokes edge waves in more general case (not only in the approximation of shallow water) replacing tangent of the beach slope, α on sine of this angle (in the shallow water approximation, these values coincide).

The main idea of analysis of appearance of the freak waves is to use the initial condition for (18) in the form of possible large impulse. Such a wave is described by the Fourier integral

$$\eta_{\mathrm{fr}}(x, y) = \eta(x, y, 0) = \int A(k) \exp\bigl(\mathrm{i}kx - |k|y\bigr)\,\mathrm{d}k, \tag{20}$$

where $A(k)$ is a spectrum of anomalous high waves. Analytical results can be easily obtained for the following spectrum

$$A(k) = \frac{A_0 l}{2} \exp\bigl(-l|k|\bigr), \tag{21}$$

where A_0 and l determine the amplitude and length of the freak wave along the shoreline. The shape of such anomalous wave is calculated from (20) analytically

$$\eta_{\mathrm{fr}}(x, y) = A_0 \frac{1 + y/l}{(1 + y/l)^2 + (x/l)^2}. \tag{22}$$

In particular, this wave on the shoreline is the Lorents-shape pulse

$$\eta_{\mathrm{fr}}(x, y = 0) = \frac{A_0}{1 + (x/l)^2}. \tag{23}$$

Thus, the freak impulse presents the crest with maximum on the shoreline (Fig. 2, dimensionless coordinates, x/l and y/l will be used in all figures); it damps more slowly in depth (as $1/y$), then along beach ($1/x^2$).

Using (22) as an initial condition, the wave field can be calculated for any time in the explicit form

$$\begin{aligned}
\eta(x, y, t) = \frac{A_0 l\sqrt{g\alpha}}{4\sqrt{((l+y)^2 + x^2)^3}} \Biggl[& \frac{4\sqrt{(l+y)^2 + x^2}\,(l+y)}{\sqrt{g\alpha}} \\
& + \mathrm{i}\sqrt[4]{\bigl((l+y)^2 + x^2\bigr)^3}\, t\sqrt{\pi} \exp\left(-\frac{t^2 g\alpha(l+y)}{4((l+y)^2 + x^2)}\right) \\
& \times \left\{ \exp\left(-\frac{3\mathrm{i}}{2}\operatorname{atan}\frac{x}{l+y} + \frac{\mathrm{i}t^2 g\alpha x}{4((l+y)^2 + x^2)}\right)\left(1 + \operatorname{erf}\left(\frac{\mathrm{i}}{2}\frac{t\sqrt{g\alpha}\exp(-\frac{\mathrm{i}}{2}\operatorname{atan}\frac{x}{l+y})}{\sqrt[4]{(l+y)^2 + x^2}}\right)\right)\right. \\
& \left. - \exp\left(\frac{3\mathrm{i}}{2}\operatorname{atan}\frac{x}{l+y} - \frac{\mathrm{i}t^2 g\alpha x}{4((l+y)^2 + x^2)}\right)\left(1 + \operatorname{erf}\left(-\frac{\mathrm{i}}{2}\frac{t\sqrt{g\alpha}\exp(\frac{\mathrm{i}}{2}\operatorname{atan}\frac{x}{l+y})}{\sqrt[4]{(l+y)^2 + x^2}}\right)\right)\right\}\Biggr].
\end{aligned} \tag{24}$$

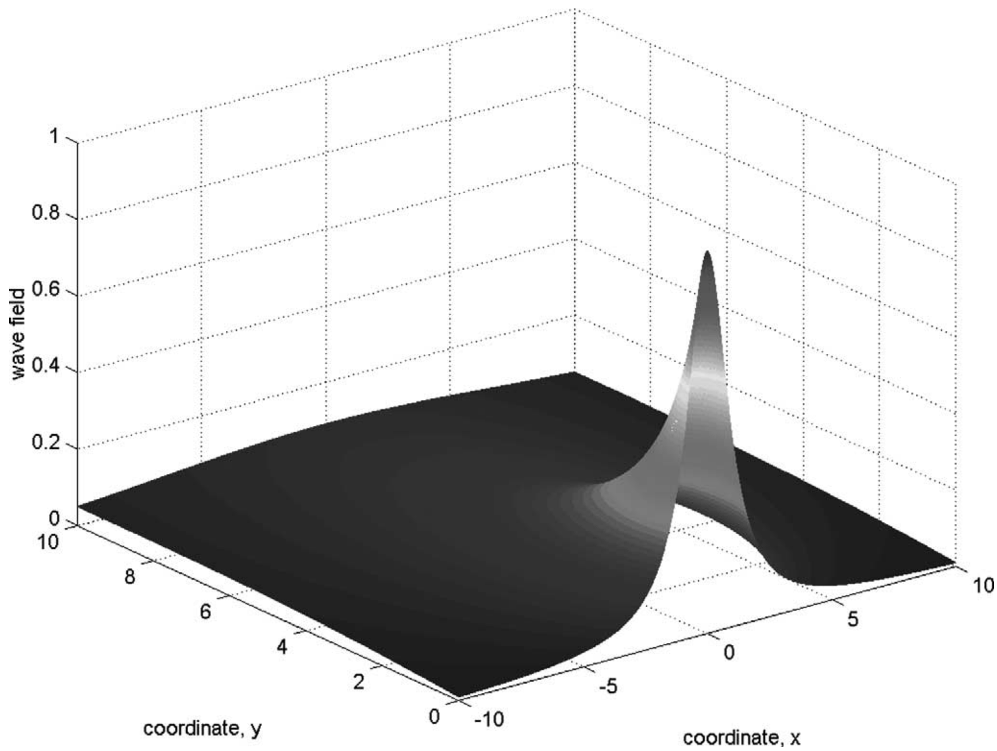

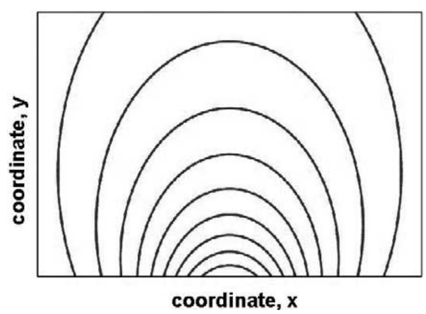

Fig. 2. Lorents pulse (22) for $n = 0$.

This solution is real. The snapshot of the wave field, η/A_0 calculated from (24) is given Fig. 3. The water displacement has the visible wave structure in alongshore direction with exponential decay in offshore direction. Main features of the wave evolution for large times can be demonstrated using the method of stationary phase

$$\eta(x, y, t) \approx \frac{A(k)}{\sqrt{2\pi t|\mathrm{d}c/\mathrm{d}k|}} \exp\bigl(\mathrm{i}(\omega t - kx - \pi/4) - |k|y\bigr), \tag{25}$$

where c is the group velocity determined by

$$c = \frac{\mathrm{d}\omega}{\mathrm{d}k} = \frac{x}{t}. \tag{26}$$

For the fixed time, the wave number as a function of coordinate, $k(x)$ is found from (26), and then the wave field from (25). After substitution of (20) and (21) these formulas are simplified

$$\eta(x, y, t) = \frac{A_0 l}{\sqrt{2\pi t\sqrt{g\alpha}}} k^{3/4} \exp(-kl - ky) \cos(\omega t - kx - \pi/4), \tag{27}$$

$$k(x, t) = \frac{g\alpha t^2}{4x^2}. \tag{28}$$

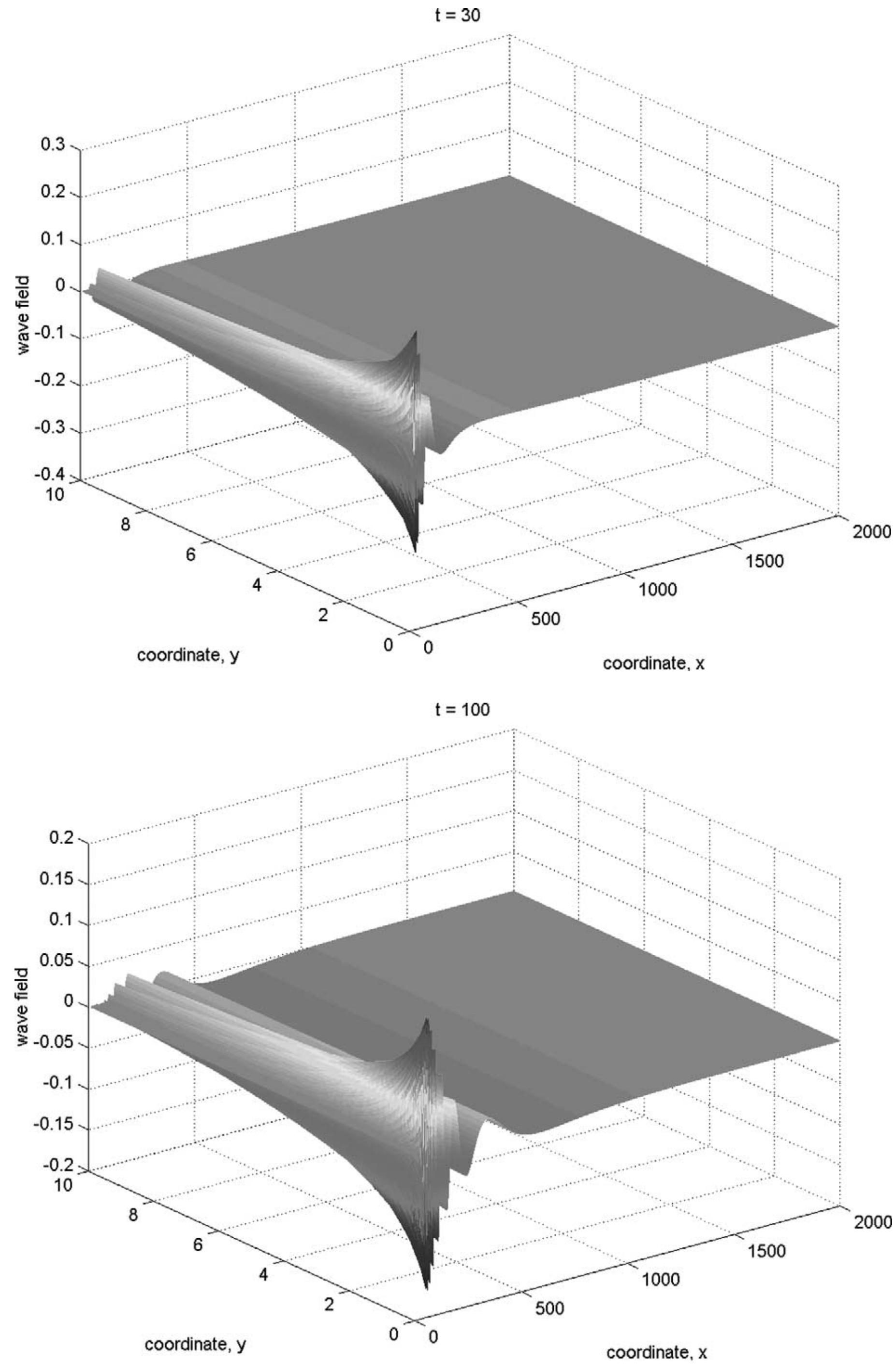

Fig. 3. Snapshot of the wave field described by (24), dimensionless time is $t(g\alpha/l)^{1/2}$.

So, the Stokes edge wave for large times presents the wave train modulated on the amplitude and wave number; its envelope shape is shown in Fig. 4 ($y = 0$, dimensionless offshore coordinate $2x/t(g\alpha l)^{1/2}$, and the amplitude is normalized on its maximum). The long waves having the large group velocity are in the front of the more short waves. The amplitude of the long

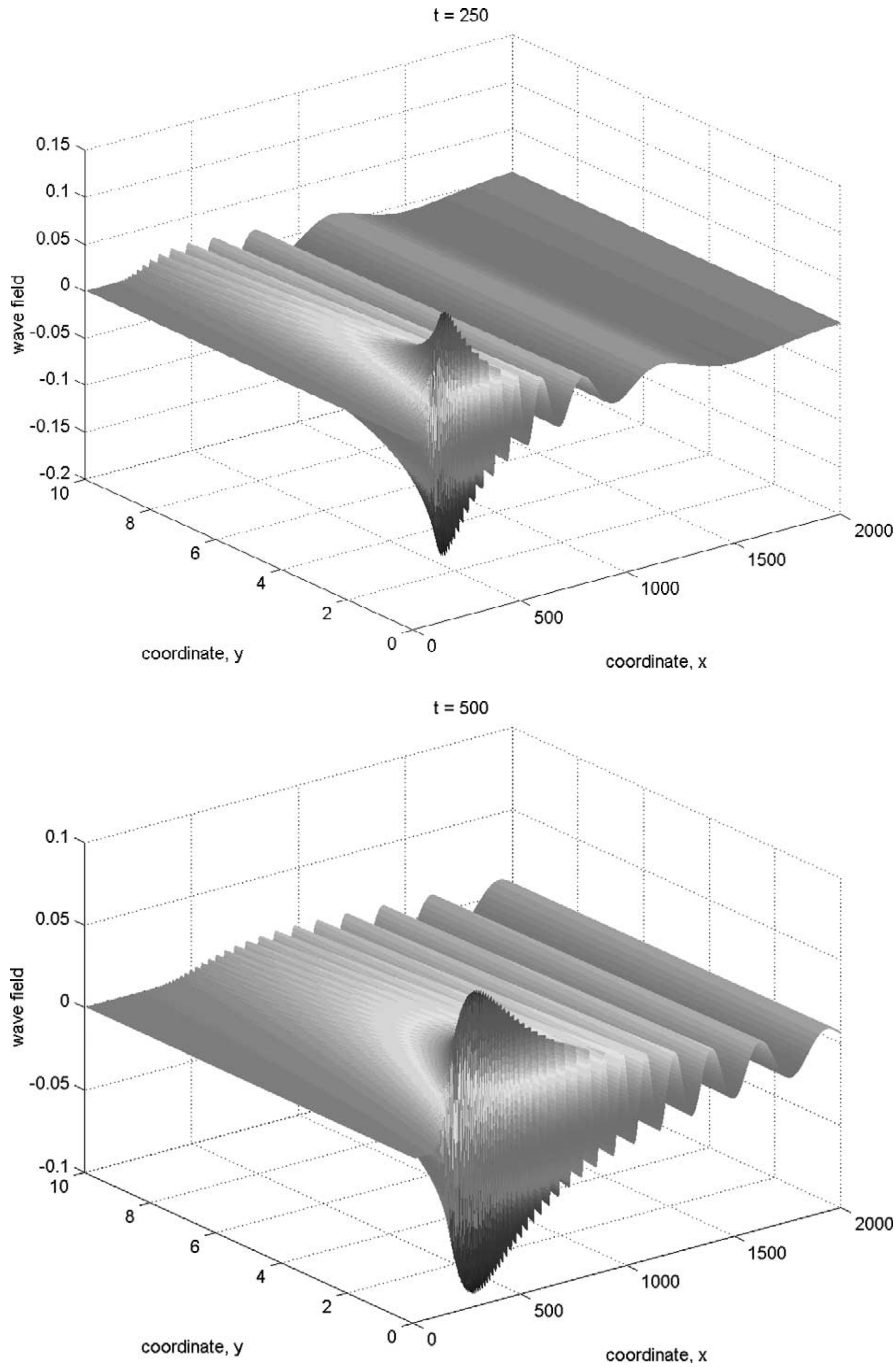

Fig. 3. (Continued).

waves is weak due to factor, $k^{3/4}$ in (27); it is also weak for the short waves due to exponential factor in (27). The maximal value of the amplitude is reached for the waves with wave number

$$k_{\max} = \frac{3}{4(l+y)}, \tag{29}$$

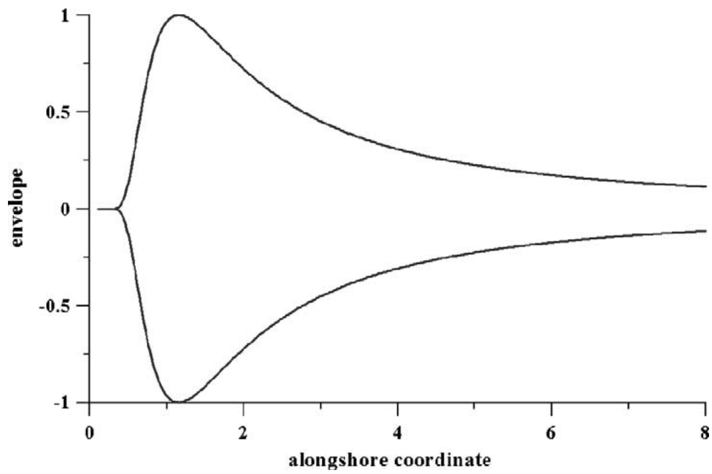

Fig. 4. Envelope shape at large times (dimensionless variables).

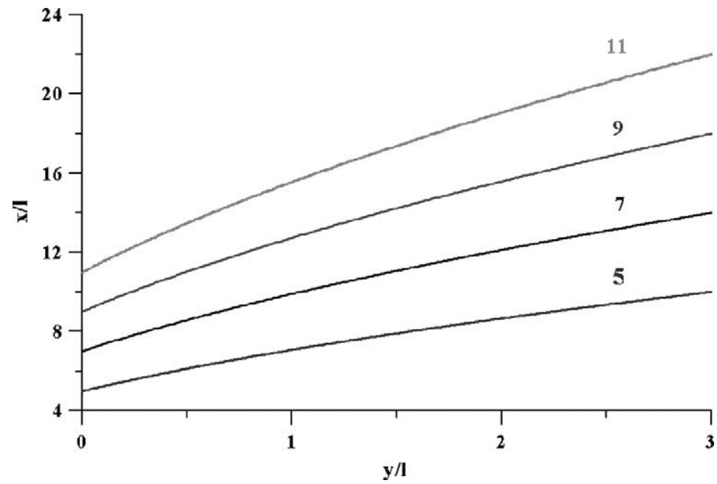

Fig. 5. Locations of the wave front for different times (dimensionless time, $t(g\alpha/3l)^{1/2}$).

and it is equal to

$$A_{\max} = \frac{A_0 l \exp(-3/4)}{\sqrt{2\pi t\sqrt{g\alpha}}}\left(\frac{3}{4(l+y)}\right)^{3/4}. \tag{30}$$

As it is expected, maximal amplitude of the wave train decreases and its length $(1/k_{\max})$ increases from the shoreline. Maximal amplitude decreases also with time due to dispersion. It is important to mention that waves in the vicinity of the maximal amplitude propagate with constant group velocity depending from the distance from shoreline

$$c_{\max} = \sqrt{\frac{g\alpha(l+y)}{3}}. \tag{31}$$

As a result, wave front in the vicinity of the maximal amplitude transforms into parabola varied with time (Fig. 5)

$$(x-x_0)^2 = \frac{g\alpha t^2}{3}(l+y). \tag{32}$$

Thus, the solitary pulse (22) transforms into the system of propagated localized "spots" of the different signs, and the spatial structure of the wave field is complicated (curvilinear fronts, damping with distance from the shoreline).

Inverting time, t and coordinate, x in (24), the wave packet will have now the slow waves on its front and fast waves in back; the wave shape is shown in Fig. 6 for dimensionless time, $t(g\alpha/l)^{1/2} = 500$, and its envelope – in Fig. 7. Such wave

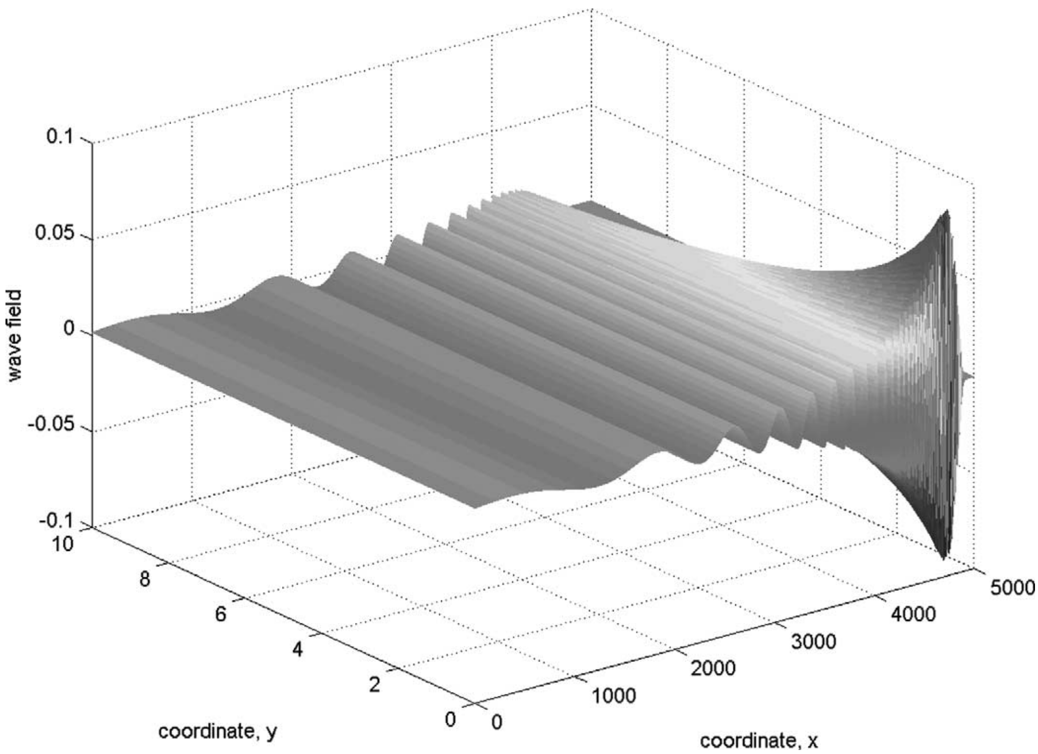

Fig. 6. Shape of the wave packet transformed in the solitary pulse (22), dimensionless time is $t(g\alpha/l)^{1/2} = 500$.

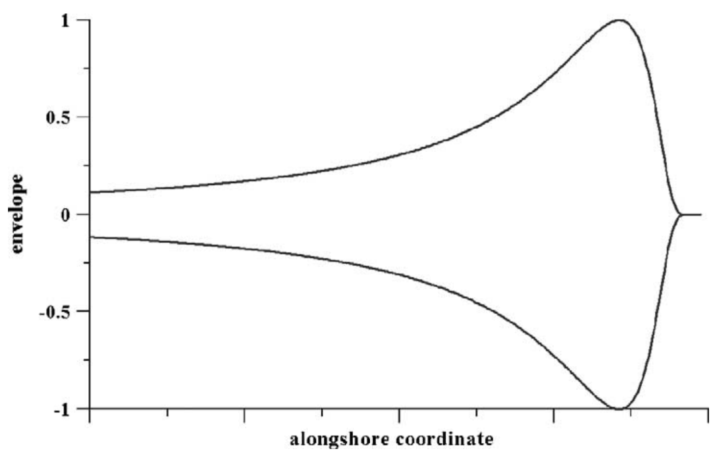

Fig. 7. The envelope shape of the wave train transformed in the solitary pulse (22).

packet will evolve with time in the localized large pulse (22), and then disperse in the wave packet shown early in Fig. 3. Fast long waves will be again in front of more slow short waves. The time variation of the maximal amplitude in the wave train calculated from (24) is presented in Fig. 8 (time is normalized on $(l/g\alpha)^{1/2}$). It is evident, that the significant amplification is in the vicinity of the wave focusing only; so, the anomalous high wave is rapidly appeared and also rapidly disappeared, and it has short-lived time.

Generally speaking, the freak wave can have any shape, not only the crest as it is considered above. A deep trough in the coastal zone may be also danger for the ship mooring. To consider the forming of the deep trough in the framework of the linear theory is trivial task because it reduces to changing of the sign of the wave amplitude, A_0. Sometimes, the freak wave may consist from highest crest and deepest trough simultaneously. The model of such an anomalous wave can be the sign-variable localized pulse (Fig. 9)

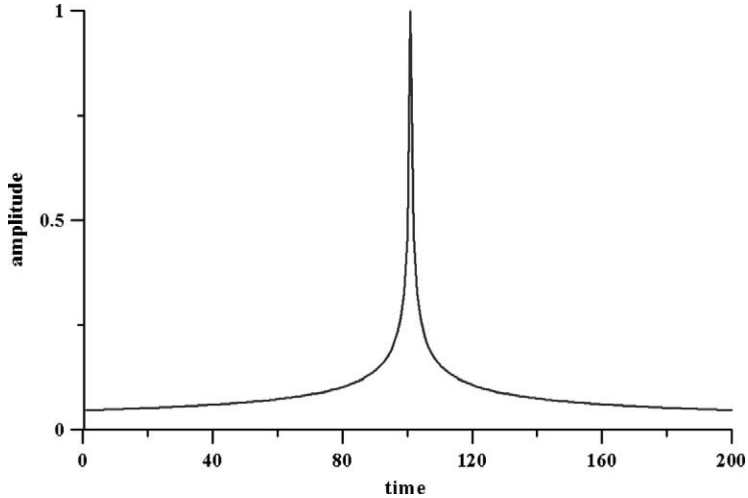

Fig. 8. Maximal value of the amplitude of the wave train versus time.

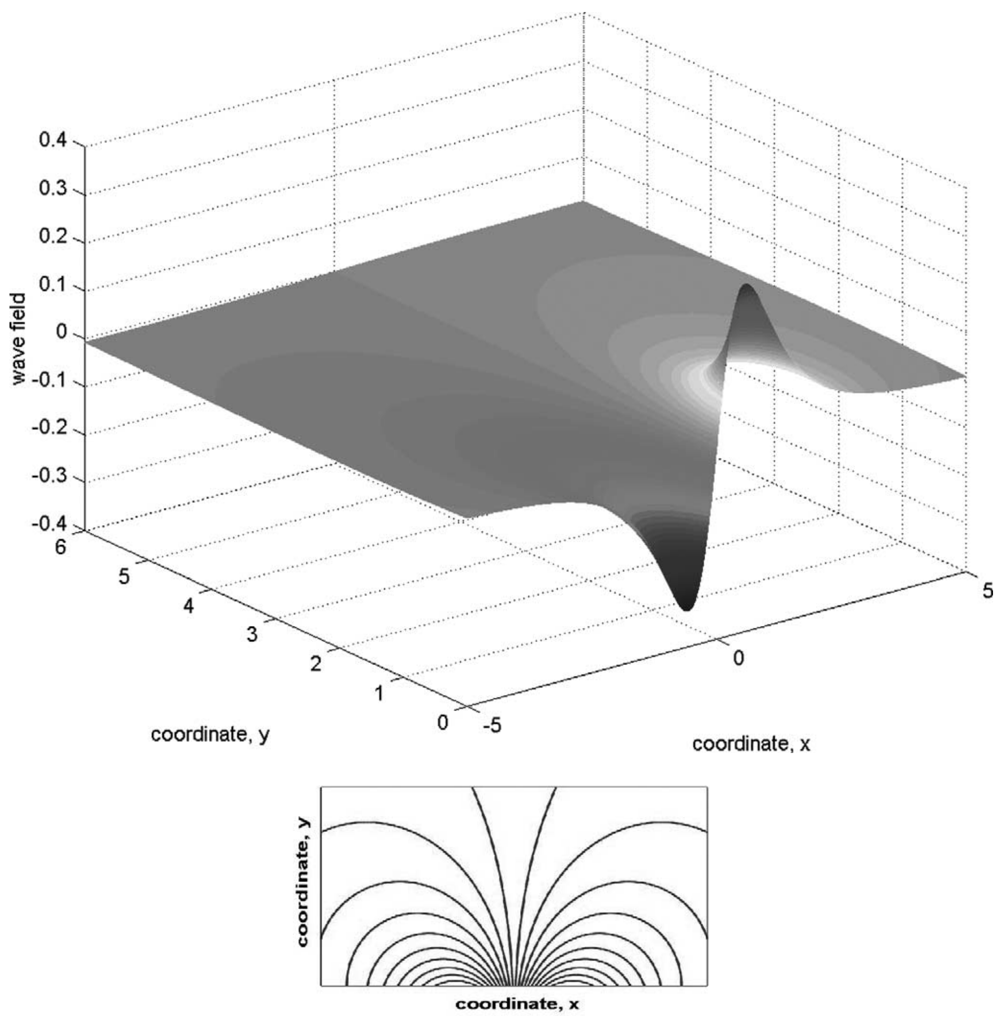

Fig. 9. The shape of the localized sign-variable pulse (33).

$$\eta_{\mathrm{fr}}(x,y)=A_0 l^2\frac{x(l+y)}{[x^2+(l+y)^2]^2}, \tag{33}$$

its spectrum according to (20) is

$$A(k)=-\frac{\mathrm{i}A_0 l^2 k}{4}\exp\bigl(-|k|l\bigr). \tag{34}$$

To find the wave trains evolved into the freak impulse can be done on the scheme described above; to calculate the Fourier integral (18) with an initial condition (33) and to invert time and coordinate in the obtained solution. It is evident that the qualitative characteristics of the wave packet for large times are the same as in Fig. 3. The quantitative characteristics are slightly different; in particular, the wave of maximal amplitude has the biggest wave number, compare with (29)

$$k_{\max}=\frac{7}{4(l+y)}. \tag{35}$$

Maximal amplitude of the wave train is

$$A_{\max}=\frac{A_0 l\exp(-7/4)}{\sqrt{2\pi t\sqrt{g\alpha}}}\left(\frac{7}{4(l+y)}\right)^{7/4}. \tag{36}$$

The wave packet, as well as the anomalous wave, damp with the offshore distance more rapidly.

5. Multi-modal field of the Stokes edge waves

The anomalous high wave can be formed by the multi-modal field of the Stokes edge waves. Let us consider firstly the Stokes edge waves with fixed modal number n. The wave field is described by the following Fourier integral

$$\eta_n(x,y,t)=\int_{-\infty}^{+\infty}A(k)L_n\bigl(2|k|y\bigr)\exp\bigl(-|k|y\bigr)\exp\bigl(\mathrm{i}(\omega t-kx)\bigr)\,\mathrm{d}k. \tag{37}$$

As an initial condition, the freak wave shape can be applied. If for instance, its spectrum is described by (21), the integral (37) can be calculated in explicit form, and the freak pulse of n-mode is (all calculations were done using MAPLE 6)

$$\eta_{\mathrm{fr}}(x,y,n=1)=A_0 l\frac{l^3-ly^2+yl^2-y^3+x^2l+3yx^2}{((l+y)^2+x^2)^2}, \tag{38}$$

$$\begin{aligned}\eta_{\mathrm{fr}}(x,y,n=2)=A_0 l\frac{1}{((l+y)^2+x^2)^3}\bigl\{&yl^4-2l^3y^2-2l^2y^3+ly^4-10y^3x^2+5yx^4\\&+x^4l-6lx^2y^2+2l^3x^2+l^5+y^5+6l^2yx^2\bigr\},\end{aligned} \tag{39}$$

$$\begin{aligned}\eta_{\mathrm{fr}}(x,y,n=3)=A_0 l\frac{1}{((l+y)^2+x^2)^4}\bigl\{&-y^6l-y^7-9yx^2l^4+7yx^6-22y^3x^4-6y^2x^2l^3+6y^3x^2l^2\\&+9y^4x^2l-11l^3x^4+6l^5x^2+x^6l+yl^6-3l^5y^2-3l^5x^2+9yl^2x^4+l^7\\&+14x^4l^3+6yx^4l^2+3y^5x^2-30y^2x^4l+3y^5l^2+3y^4l^3+18y^5x^2-3y^3l^4\\&+6y^4lx^2-36y^3l^2x^2-13y^3x^4+15y^2lx^4-12l^3y^2x^2+18yl^4x^2\bigr\},\end{aligned} \tag{40}$$

$$\begin{aligned}\eta_{\mathrm{fr}}(x,y,n=4)=A_0 l\frac{1}{((l+y)^2+x^2)^5}\bigl\{&x^4y^5-6l^7x^2-4l^6y^3+6l^4y^5+6l^5y^4-4l^2y^7-4l^7y^2\\&-4l^3y^6+10l^7x^2+l^9+120ly^4x^4-10ly^2x^6-6y^7x^2+80y^5x^4-70y^3x^6\\&-4lx^8+4yx^8+l^8y-18ly^6x^2+70l^2x^6y-160l^3x^4y^2+10l^3x^6+25l^4x^4y\\&+30l^6x^2y-80l^2x^4y^3-30y^7x^2+ly^8-10ly^6x^2-55ly^4x^4+4l^3x^6+30l^3y^4x^2\\&+90l^3y^2x^4-90l^4y^3x^2-30l^5y^2x^2+90l^2y^5x^2-70l^2y^3x^4+30l^3x^2y^4\\&-18l^6x^2y+30l^4x^2y^3-6l^5x^2y^2+40l^5x^4-6l^2x^2y^5-4y^3x^6+45y^5x^4+y^9\\&+5x^8y+5x^8l-10x^6l^3+5x^4ly^4+5l^4x^4y+10l^2x^4y^3+10l^3x^4y^2-10x^6y^3\\&+x^4l^5-18lx^6y^2-42l^2x^6y-35l^5x^4\bigr\}.\end{aligned} \tag{41}$$

It is important to mention that all integrals on the shoreline ($y = 0$) for any modal number n reduce to the Lorents-shape pulse (23). When the offshore distance increases, the impulse consists from the crests and troughs due to sign-variability of the Laguerre polynomials. Computed freak wave shape for several modal numbers, n is shown in Fig. 10. The oscillatory wave structure on the freak wave periphery is clearly seen for large modal numbers.

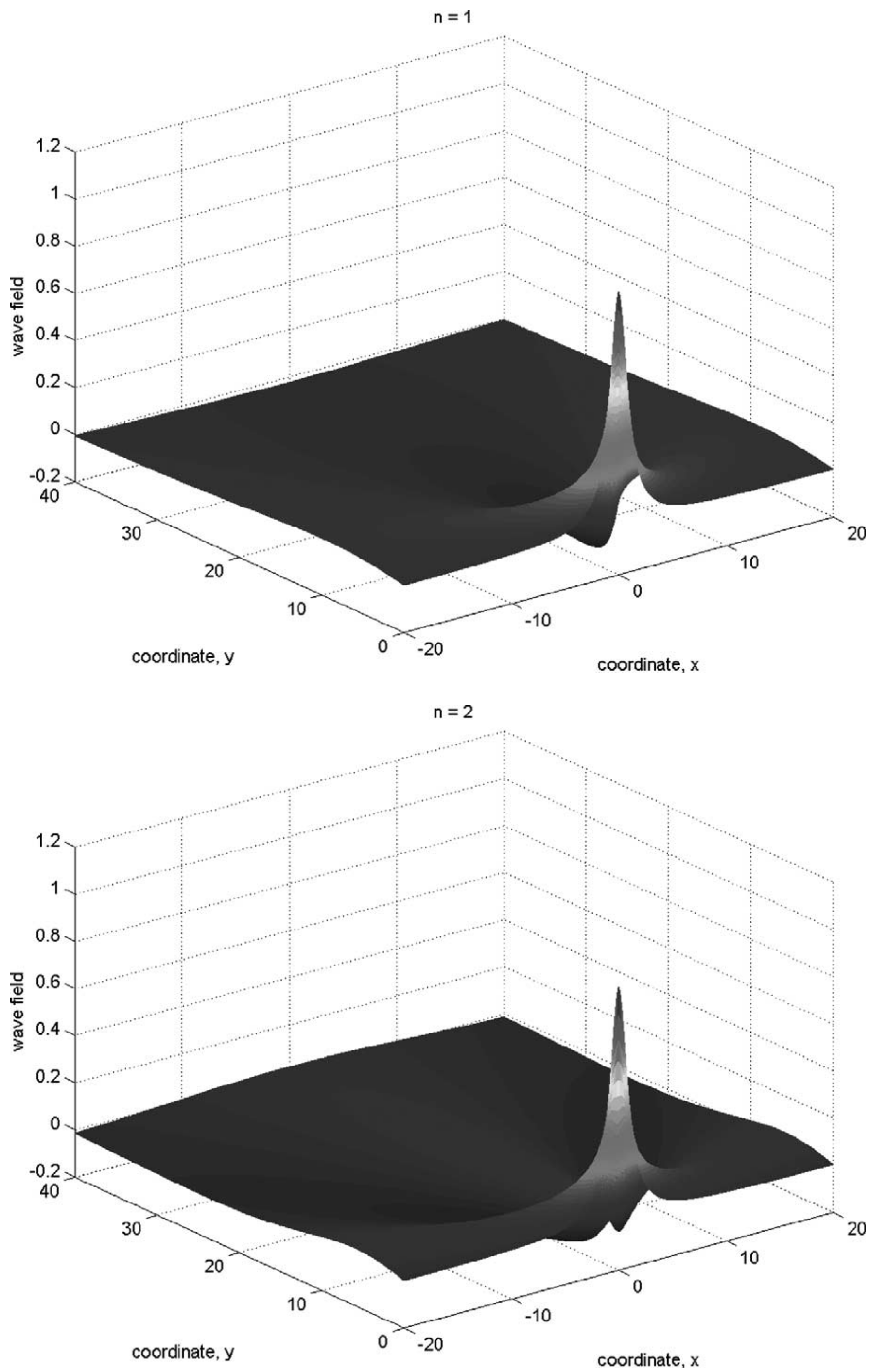

Fig. 10. Freak wave shape for different modal number (the same spectrum).

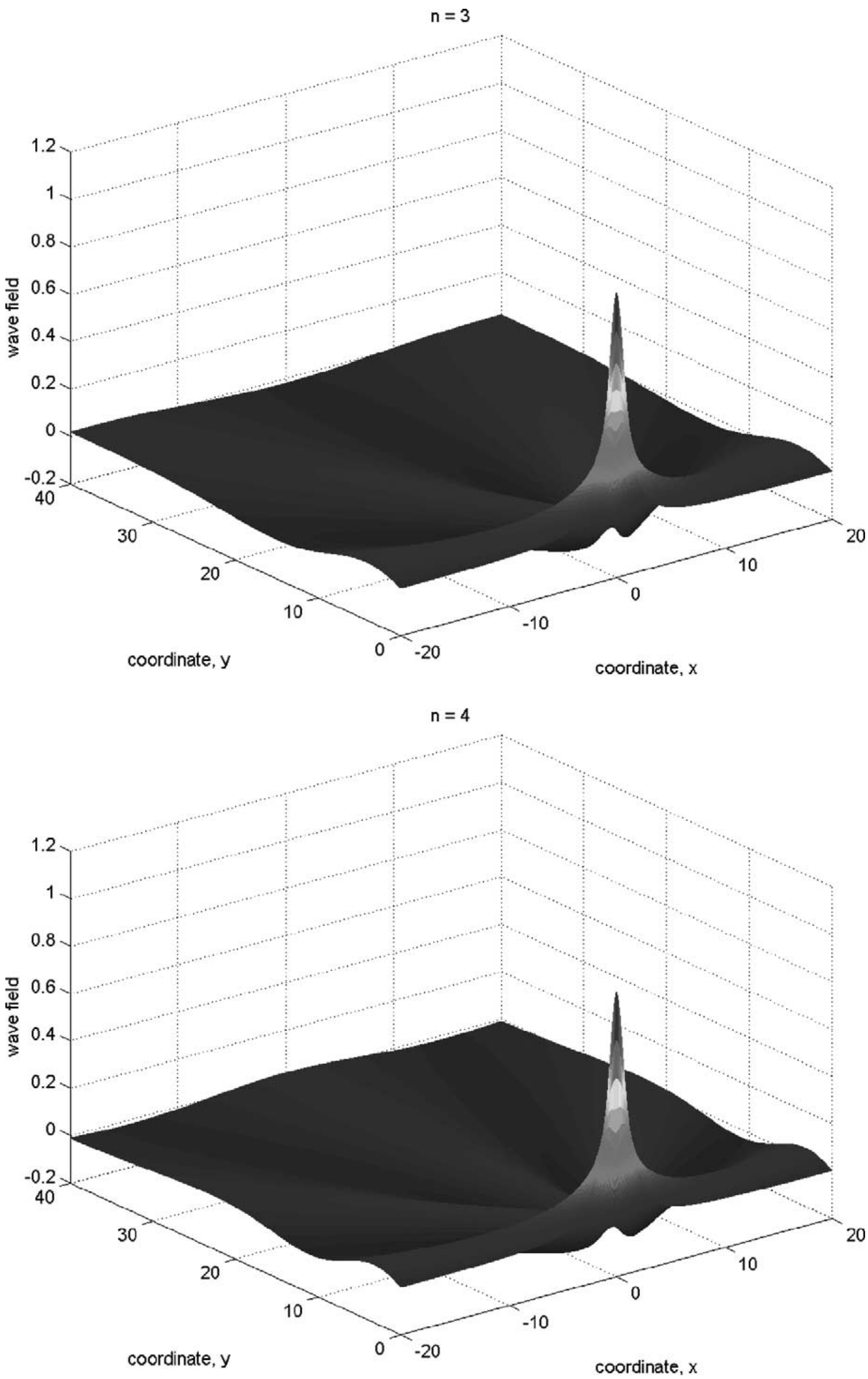

Fig. 10. (Continued).

For large time, the stationary phase method is effective to calculate the wave field. Along the beach ($y = 0$) the wave field is described by the asymptotic formulas (26)–(29) replacing the gravity acceleration, g with $g(2n+1)$. As a result, the maximal amplitude of the wave packet of n-mode is

$$A_{\max} = \frac{A_0 l \exp(-3/4)}{\sqrt{2\pi t\sqrt{g\alpha(2n+1)}}}\left(\frac{3}{4l}\right)^{3/4}, \tag{42}$$

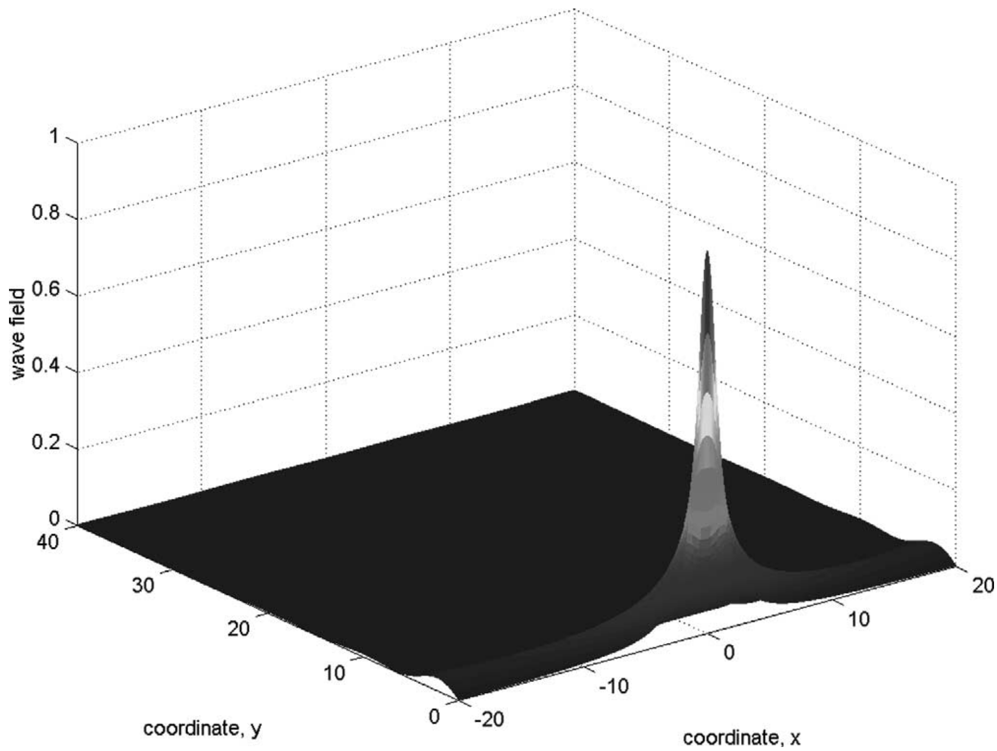

Fig. 11. Shape of the freak wave consisted from 11 modes with the same spectrum.

and it decreases when the modal number increases. The characteristic wavelength does not depend from the modal number and it is determined by (27). The group velocity of the wave packet of the maximal amplitude increases when the modal number increases

$$c_{\mathrm{gr}} = \sqrt{\frac{gl\alpha(2n+1)}{3}}. \tag{43}$$

Due to linearity of the shallow water equations it is easily to consider the freak wave formation in the multi-modal field of the Stokes edge waves. If for instance the freak wave consists from the eleven modes with the same spectrum (20), then anomalous impulse is very narrow and it is located in the vicinity of the shoreline. It is shown in Fig. 11. With time, this freak wave evolves in the system of the eleven oscillatory packets with the leading weak amplitude packet of the highest mode; see Fig. 12 for dimensionless time, $t(g\alpha/l)^{1/2} = 500$. Inverting time and alongshore coordinate, such a multi-modal wave packet will evolve in the large amplitude impulse, and then again disperse.

6. Conclusion

The main result of this study is the demonstration of possibility of the freak wave phenomenon in the field of the trapped waves in the coastal zone. Because the long shelf waves can be excited by the nonlinear interaction of the wind wave groups, the opportunity of the appearance of the large-scale anomalous wave at the variable wind seems to be important. The physical reasons of the appearance of the large-amplitude waves may be related also with the processes of the multi-generation of waves, for instance, at the underwater earthquakes and volcano. The problem of the spatial localization of the freak wave formed from the Stokes edge wave field is solved naturally because the wave field decreases when the offshore distance increases. This is main difference to compare with the wind wave field, which propagates in both horizontal coordinates. The freak wave can present the impulse of any shape: high crest only, deep trough only, or the system of crests and troughs. Far from the focal point (caustics) the wave field is the frequency (phase) modulated wave packet with weak amplitudes, or the system of such packets with different offshore structure (different modal numbers). Its spatial structure is complicated enough, for instance, the front of the wave of maximal amplitude presents the parabola in space and so on.

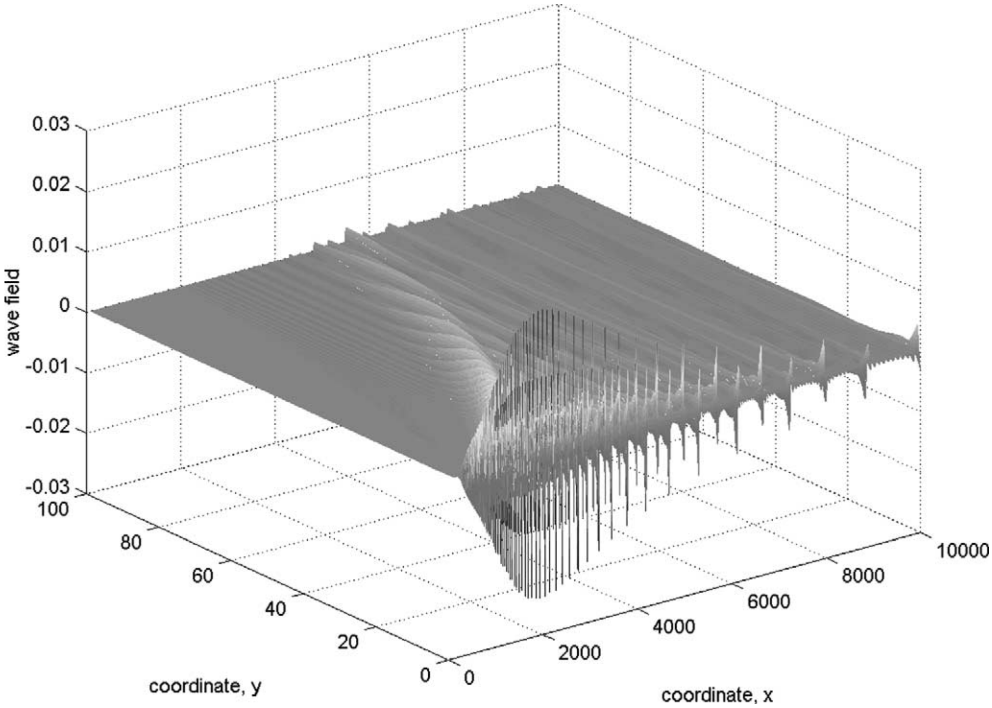

Fig. 12. Wave train consisted from 11 modes with the same spectrum, dimensionless time is $t(g\alpha/l)^{1/2} = 1000$.

Deterministic Stokes edge waves are considered above. In the framework of the linear theory the random and regular components propagate independently. As a result, the freak wave may be formed on the background of the random sea. Recent investigations in the framework of the weak nonlinear theory (like Korteweg–de Vries and nonlinear Schrödinger equations) shown that the freak wave forms in the random wind wave field [26,28]. The main weak nonlinear effect for the collinear Stokes waves is modulation instability [36], nonlinear interaction between different modes is absent in the first approximation [39]. Some exact solutions of the nonlinear governing equations described a family of explicit rotational waves are obtained [42]. We plan to study numerically the nonlinear process of the focusing of the edge waves taking into account the random background wave field later.

Acknowledgement

This study is supported particularly by the INTAS grants (99-1068 and 01-2156), and RFBR grants (00-05-64922 and 02-05-65107).

References

[1] H. Ishii, K. Abe, Propagation of tsunami on a linear slope between two flat regions, I. Eigenwave, J. Phys. Earth 28 (1980) 531–541.
[2] Yu.I. Shokin, L.B. Chubarov, A.G. Marchuk, K.V. Simonov, Numerical Experiment in the Tsunami Problem, Nauka, Novosibirsk, 1988.
[3] E.N. Pelinovsky, Hydrodynamics of Tsunami Waves, Applied Physics Institute Press, Nizhny Novgorod, 1996.
[4] I.V. Fine, G.V. Shevshenko, E.A. Kulikov, The study of trapped properties of the Kurile shelf by the ray methods, Oceanology 23 (1) (1983) 23–26.
[5] Y.M. Tang, R. Grimshaw, A modal analysis of coastally trapped waves generated by tropical cyclones, J. Phys. Oceanogr. 25 (1995) 1577–1598.
[6] R.T. Guza, R.E. Davis, Excitation of edge waves by waves incident on a beach, J. Geophys. Res. 79 (1974) 1285–1291.
[7] M.A. Foda, C.C. Mei, Nonlinear excitation of long trapped waves by a group of short swell, J. Fluid Mech. 111 (1981) 319–345.
[8] Y. Agnon, C.C. Mei, Trapping and resonance of long shelf waves due to groups of short waves, J. Fluid Mech. 195 (1988) 201–221.
[9] P. Komar, Beach Processes and Sedimentation, Prentice Hall, New York, 1998.
[10] F.K. Ball, Edge waves in an ocean of finite depth, Deep-Sea Res. 14 (1967) 79–88.

[11] D.V. Evans, P. McIver, Edge waves over a shelf: full linear theory, J. Fluid Mech. 142 (1984) 79–95.
[12] R. Grimshaw, Edge waves: a long wave theory for oceans of finite depth, J. Fluid Mech. 62 (1974) 775–791.
[13] W. Munk, F. Snodgrass, M. Wimbush, Tides off-shore: transition from California coastal to deep-sea waters, Geophys. Fluid Dynamics 1 (1970) 161–235.
[14] F. Ursell, Edge waves on a sloping beach, Proc. Roy. Soc. London Ser. A 214 (1952) 79–97.
[15] P. LeBlond, L. Mysak, Waves in the Ocean, in: Elsevier Oceanogr. Ser., Vol. 20, 1978.
[16] A.B. Rabinovich, Long Ocean Gravity Waves: Trapping, Resonance, Leaking, Hydrometeoizdat, St. Petersburg, 1993.
[17] H.F. Reid, S. Taber, The Virgin Islands Earthquakes of 1867–1868, Bull. Seismol. Soc. Amer. 10 (1920) 9–30.
[18] L. Graham, Monsters of the deep, New Scientist 170 (2297) (2001).
[19] S. Haver, O. Andersen, Freak waves: rare realizations of a typical population or typical realization of rare population?, in: Proc. 10th Int. Offshore and Polar Engineering Conference, Seattle, May 28–June 2, 2000, pp. 123–130.
[20] M.G. Brown, The Maslov integral representation of slowly varying dispersive wavetrains in inhomogeneous moving media, Wave Motion 32 (2000) 247–266.
[21] M.G. Brown, Space–time surface gravity wave caustics: structurally stable extreme wave events, Wave Motion 33 (2001) 117–143.
[22] K.B. Dysthe, K. Trulsen, Note on breather type solutions of the NLS as a model for freak-waves, Phys. Scripta T 82 (1999) 48–52.
[23] K.L. Henderson, D.H. Peregrine, J.W. Dold, Unsteady water wave modulations: fully nonlinear solutions and comparison with the nonlinear Schrödinger equation, Wave Motion 29 (1999) 341–361.
[24] C. Kharif, E. Pelinovsky, T. Talipova, A. Slunyaev, Focusing of nonlinear wave group in deep water, JETP Lett. 73 (4) (2001) 170–175.
[25] I. Lavrenov, The wave energy concentration at the Agulhas current of South Africa, Nat. Hazards 17 (1998) 117–127.
[26] M. Onarato, A.R. Osborne, M. Serio, S. Bertone, Freak waves in random oceanic sea states, Phys. Rev. Lett. 86 (25) (2001) 5831–5834.
[27] A.R. Osborne, M. Onorato, M. Serio, The nonlinear dynamics of rogue waves and holes in deep-water gravity wave train, Phys. Lett. A 275 (2000) 386–393.
[28] E. Pelinovsky, T. Talipova, C. Kharif, Nonlinear dispersive mechanism of the freak wave formation in shallow water, Physica D 147 (2000) 83–94.
[29] D.H. Peregrine, Interaction of water waves and currents, Adv. Appl. Mech. 16 (1976) 9–117.
[30] D.H. Peregrine, Water waves, nonlinear Schrödinger equations and their solutions, J. Austral. Math. Soc. Ser. B 25 (1983) 16–43.
[31] R. Smith, Giant waves, J. Fluid Mech. 77 (1976) 417–431.
[32] B.S. White, B. Fornberg, On the chance of freak waves at sea, J. Fluid Mech. 355 (1998) 113–138.
[33] A. Minzoni, G.B. Whitham, On the excitation of edge waves on beaches, J. Fluid Mech. 79 (1977) 273–287.
[34] G.B. Whitham, Nonlinear effects in edge waves, J. Fluid Mech. 74 (1976) 353–368.
[35] T.R. Akylas, Large-scale modulation of edge waves, J. Fluid Mech. 132 (1983) 197–208.
[36] H.H. Yeh, Nonlinear progressive edge waves: their instability and evolution, J. Fluid Mech. 152 (1985) 479–499.
[37] K.E. Kenyon, A note on conservative edge wave interactions, Deep-Sea Res. 17 (1970) 197–201.
[38] I.E. Kochergin, E.N. Pelinovsky, Nonlinear interaction of the edge waves triad, Oceanology 29 (6) (1989) 899–903.
[39] J.T. Kirby, U. Putrevu, H.T. Ozkan-Haller, Evolution equations for edge waves and shear waves on longshore uniform beaches, in: Proc. 26th Int. Conf. Coastal Engineering, 1998, pp. 203–216.
[40] G.B. Whitham, Linear and Nonlinear Waves, Wiley, 1974.
[41] L. Ostrovsky, A. Potapov, Modulated Waves. Theory and Applications, John Hopkins Press, Baltimore, 1999.
[42] A. Constantin, Edge waves along a sloping beach, J. Phys. A 34 (2001) 9723–9731.